

Cascaded dual-channel fiber SPR temperature sensor based on liquid and solid encapsulations

Yong Wei(魏勇), Lingling Li(李玲玲), Chunlan Liu(刘春兰), Jiangxi Hu(胡江西), Yudong Su(苏于东), Ping Wu(吴萍), and Xiaoling Zhao(赵晓玲)

Citation: Chin. Phys. B, 2021, 30 (**10**): 100701. DOI: 10.1088/1674-1056/ac0426
Journal homepage: http://cpb.iphy.ac.cn; http://iopscience.iop.org/cpb

What follows is a list of articles you may be interested in

A modified analytical model of the alkali-metal atomic magnetometer employing longitudinal carrier field

Chang Chen(陈畅), Yi Zhang(张燚), Zhi-Guo Wang(汪之国), Qi-Yuan Jiang(江奇渊), Hui Luo(罗晖), and Kai-Yong Yang(杨开勇)

Chin. Phys. B, 2021, 30 (**5**): 050707. DOI: 10.1088/1674-1056/abd7d3

In-situ fabrication of ZnO nanoparticles sensors based on gas-sensing electrode for ppb-level H_2S detection at room temperature

Jing-Yue Xuan(宣景悦), Guo-Dong Zhao(赵国栋), Xiao-Bo Shi(史小波), Wei Geng(耿伟), Heng-Zheng Li(李恒征), Mei-Ling Sun(孙美玲), Fu-Chao Jia(贾福超), Shu-Gang Tan(谭树刚), Guang-Chao Yin(尹广超), and Bo Liu(刘波)

Chin. Phys. B, 2021, 30 (**2**): 020701. DOI: 10.1088/1674-1056/abcf46

Fiber cladding SPR bending sensor characterized by two parameters

Chunlan Liu(刘春兰), Jiangxi Hu(胡江西), Yong Wei(魏勇), Yudong Su(苏于东), Ping Wu(吴萍), Lingling Li(李玲玲), and Xiaoling Zhao(赵晓玲)

Chin. Phys. B, 2020, 29 (**12**): 120701. DOI: 10.1088/1674-1056/aba9c1

Acetone sensors for non-invasive diagnosis of diabetes based on metal-oxide-semiconductor materials

Yujie Li(李育洁), Min Zhang(张敏), Haiming Zhang(张海明)

Chin. Phys. B, 2020, 29 (**9**): 090702. DOI: 10.1088/1674-1056/aba60b

Microfluidic temperature sensor based on temperature-dependent dielectric property of liquid

Qi Liu(刘琦), Yu-Feng Yu(俞钰峰), Wen-Sheng Zhao(赵文生), Hui Li(李慧)

Chin. Phys. B, 2020, 29 (**1**): 010701. DOI: 10.1088/1674-1056/ab593c

---

Cascaded dual-channel fiber SPR temperature sensor based on liquid and solid encapsulations*

Yong Wei(魏勇), Lingling Li(李玲玲), Chunlan Liu(刘春兰)†, Jiangxi Hu(胡江西), Yudong Su(苏于东), Ping Wu(吴萍), and Xiaoling Zhao(赵晓玲)

College of Electronic & Information Engineering, Chongqing Three Gorges University, Chongqing 404100, *China*

(Received 18 March 2021; revised manuscript received 19 May 2021; accepted manuscript online 24 May 2021)

In order to control the working wavelength range of the fiber surface plasmon resonance (SPR) temperature sensor and realize the wavelength division multiplexing type multi-channel fiber SPR temperature sensor, by comprehensively investigating the influence of liquids with different thermal-optical coefficients and solid packaging materials on the performance of fiber SPR temperature sensor, a dual-channel fiber SPR temperature sensor based on liquid–solid cascade encapsulation was designed and fabricated. The liquid temperature sensing stage encapsulated in capillary worked in 616.03 nm–639.05 nm band, the solid sensing stage coated with pouring sealant worked in 719.37 nm–825.27 nm band, and the two stages were cascaded to form a fiber dual-channel temperature sensor. The testing results indicated that when the temperature range was 35 °C–95 °C, the sensitivity of two-stage temperature detection was −0.384 nm/°C and −1.765 nm/°C respectively. The proposed fiber sensor has simple fabrication and excellent performance which can be widely used in various fields of dual-channel temperature measurement and temperature compensation.

Keywords: surface plasmon resonance (SPR), temperature sensor, liquid–solid cascade, dual channel

PACS: 07.07.Df, 42.81.Cn, 71.45.Gm **DOI:** 10.1088/1674-1056/ac0426

1. Introduction

As a very important physical parameter, temperature has the detection demand in the fields of food, medicine, architecture, and oil, sensors for temperature detection and compensation emerge in endlessly.[1–3] Fiber sensor has attracted wide attention due to its small size, high sensitivity, anti-electromagnetic interference, and can be used in harsh environment. Fiber Mach Zehnder interferometer (MZI) used for temperature measurement has been developed gradually by scholars.[4–6] The MZI temperature sensor fabricated by femtosecond lase[7,8] has a wide range of temperature measurement and a little higher sensitivity. However, it also has problems of expensive manufacturing equipment, complex manufacturing process, and easy to break. The Fabry–Pérot interferometer (FPI) temperature sensor[9,10] can work at high temperatures, but its processing equipment is expensive and its manufacturing process is complex. Fiber Bragg grating (FBG) temperature sensor has been widely used, but its sensitivity is low, usually at the level of pm.[11,12] Although the temperature sensitivity of long period fiber grating (LPFG) temperature sensor[13–15] has been improved, it has the problem of cross sensitivity because that it is sensitive to multiple parameters.

In recent years, fiber temperature sensor based on SPR mechanism has attracted much attention. Zhu[16] employed the ground dual-core fiber coated with polydimethylsiloxane (PDMS) to fabricate the reflected fiber temperature sensor, the sensitivity with the detection range of 20 °C–70 °C reached 3.1 nm/°C. However, it is difficult to obtain the special fiber and grind bare optical fiber. Zhao *et al.*[17] employed silver mirror reaction to coat silver film on the thick core fiber with the core diameter of 600 μm, and packaged the fiber in a glass capillary filled with alcohol to realize the temperature sensor. The sensitivity with the detection range of 70 °C–35 °C reached −1.5745 nm/°C, however, the sensing probe was fabricated by the fiber with a non-standard core diameter, and silver mirror reaction process was not easy to control accurately. By employing hollow fiber filled with liquid crystal, Peng and his team[18] fabricated fiber SPR temperature sensor. The sensitivity was 4.72 nm/°C with detection range of 20 °C–34.5 °C which realized the detection of the solution with the high refractive index. However, it is difficult to coat silver film on the inner wall of fiber, and the temperature measurement range of the sensor is narrow.

The fiber SPR temperature sensors mentioned above are all single-stage and single-channel temperature sensors, which cannot realize multi-channel temperature measurement and temperature compensation. And there are few teams to study

*Project supported by the National Natural Science Foundation of China (Grant No. 61705025), the Natural Science Foundation of Heilongjiang Province, China (Grant No. F2018027), partially supported by Chongqing Natural Science Foundation (Grant Nos. cstc2019jcyj-msxmX0431 and cstc2018jcyjAX0817), the Science and Technology Project Affiliated to the Education Department of Chongqing Municipality (Grant Nos. KJQN201801217, KJQN201901226, and KJ1710247), Chongqing Key Laboratory of Geological Environment Monitoring and Disaster Early-Warning in Three Gorges Reservoir Area (Grant Nos. ZD2020A0103 and ZD2020A0102), and the Fundamental Research Funds for Chongqing Three Gorges University of China (Grant No. 19ZDPY08).

†Corresponding author. E-mail: lclliuchunlan@163.com

© 2021 Chinese Physical Society and IOP Publishing Ltd

the influence of encapsulation materials with different refractive indexes and thermal-optical coefficients on the resonance wavelength, dynamic range, sensing sensitivity, and response time of SPR temperature sensor. Based on these, we studied the effect of the distilled water, sodium chloride solution, sucrose solution, calcium chloride solution, and glycerol solution with different thermal-optical coefficients and refractive indexes on the resonance wavelength, dynamic range, sensing sensitivity, and response time of SPR temperature sensor. The results indicated that the distilled water worked in short wavelength range and the pouring sealant worked in long wavelength range. According to the WDM dual-channel sensing principle, a dual-channel fiber SPR temperature sensor scheme based on liquid–solid cascaded encapsulation is proposed, Finally, we employed the distilled water liquid encapsulation stage with the lowest refractive index and potting glue solid encapsulation stage to realize the dual-channel fiber SPR temperature sensor.

2. Sensing probe structure and fabrication

The classical application of fiber SPR sensor is the detection of refractive index. When the refractive index of the external environment changes, the resonance wavelength of the fiber sensor will move in a large range, so the corresponding relationship between the resonance wavelength and the refractive index is built, and high sensitivity refractive index sensing is carried out The fiber temperature sensor based on SPR mechanism needs to be coated outside the sensing film with a encapsulation material which has a large thermal-optical coefficient to provide an refractive index environment varying with the temperature. Due to the influence of the thermal-optical coefficient of the encapsulation material, the refractive index of the encapsulation material is different at different temperatures, then the resonance wavelength of the sensing probe is different. By constructing the corresponding relationship between SPR resonance wavelength and ambient temperature, the fiber SPR temperature sensor is realized. Based on this, we proposed a transmission-type SPR temperature sensing probe sealed in the silica capillary filled with liquid, figure 1(a) shows the practicality picture of the sensing probe, and figure 1(b) is the structure diagram. By employing the plastic cladding quartz core multimode optical fiber whose cladding is easy to strip mechanically, mechanically stripping the cladding and coating layer as the sensing zone, coating 50-nm sensing gold film outside the sensing zone rotatably, and placing the sensing probe in the silica capillary filled with liquid, thus the fiber SPR temperature sensor was fabricated. The wide spectrum light was injected from the left side of the plastic clad multimode fiber, and the SPR effect occurred when it contacted with the 50-nm sensing gold film in the sensing area. The light signal after the SPR effect transmitted along the right side of the fiber to the spectrometer for detection. When the ambient temperature changes, the temperature of the liquid encapsulation material in the capillary changes with it. Affected by the thermo-optical coefficient, the refractive index of the liquid encapsulation material changes correspondingly, which leads to the shift of the resonance wavelength, and then the corresponding relationship between SPR resonance wavelength and temperature is established, thus the temperature sensing is realized. Besides that, the liquid encapsulation of fiber optic probe can effectively avoid the evaporation of liquid in the process of long-term use and temperature change.

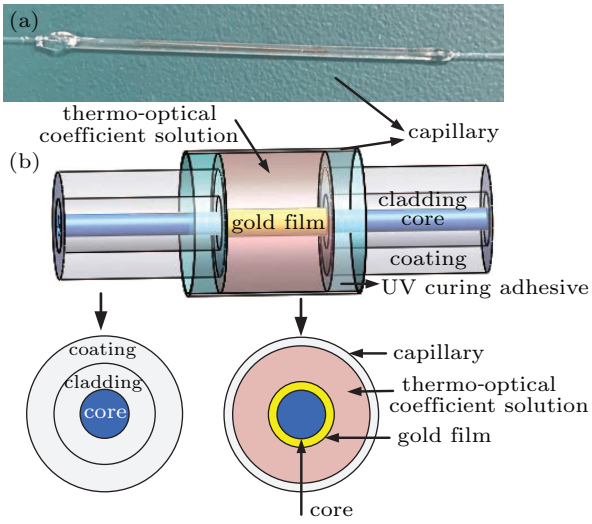


Fig. 1. Liquid-encapsulated fiber SPR temperature sensor, (a) practicality picture, (b) schematic diagram.

The fabrication process of liquid-encapsulated fiber SPR sensor is described below:

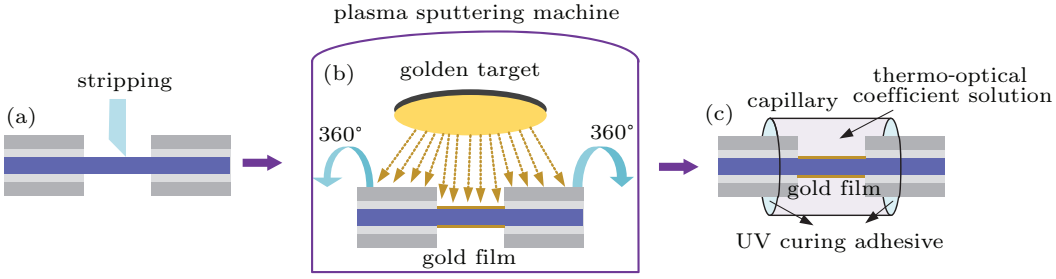


Fig. 2. The fabrication of the liquid-encapsulated fiber SPR temperature sensor, (a) mechanical stripping of coating and plastic cladding, (b) ring plating of 50-nm gold film, (c) quartz capillary liquid encapsulation.

Firstly, by taking a plastic clad multimode fiber (PTIF125/140/250HT37, NewPion Photonics) with the core diameter of 125 μm, mechanically peelling off the coating and plastic cladding in the middle of the fiber, and the quartz core with the length of 2 cm was exposed, as shown in Fig. 2(a).

Secondly, the fiber was put into the rotary clamping device of plasma sputtering instrument (ETD-2000, YLBT), the bare part of the fiber core was placed directly below the gold target, and the two ends of the fiber were fixed by the optical fiber clamp with a rotating motor. In the process of coating, the motor drove the clamp to rotate in a circle, and the 50-nm gold film was uniformly coated on the side of the fiber as shown in Fig. 2(b). The thickness of the gold film was monitored by the film thickness monitor.

Finally, the fiber probe after gold coating was inserted into a 5-cm long quartz capillary tube with inner and outer diameters of 150 μm and 360 μm respectively. The encapsulation solution was injected into the capillary tube with a micro flow pump, and the two ends of the capillary tube were dot coated with UV curing adhesive, as shown in Fig. 2(c). In order to confirm that the sealed liquid will not leak or evaporate, the capillary tube was inserted into the tee, the two ends of the tee are sealed with industrial rubber paste, the upper end of the tee is connected with the syringe by a hose, and the syringe was pushed by a micro flow pump to fill the capillary tube with the liquid to be measured. After that, the industrial rubber paste and the tee were removed, and the gap between the capillary tube and the fiber was sealed with UV curing adhesive to ensure that the solution will not leak or evaporate.

3. Research on thermal-optical coefficient of liquid encapsulation materials and simulation of temperature sensing performance

The liquid encapsulation materials with different refractive indexes and thermal-optical coefficients will make the dynamic range of resonance wavelength and sensitivity of fiber SPR temperature sensor different. In order to control the working wavelength range of the SPR temperature sensor, divide two working wave bands in the limited bandwidth of light source spectrometer, and then realize the wavelength division multiplexing dual-channel fiber SPR temperature sensor. It is necessary to study the thermal-optical coefficient of liquid encapsulation materials, and then simulate the influence on the performance of optical fiber SPR temperature sensor according to the research results of thermal-optical coefficient.

3.1. Research on the thermal-optical coefficient of liquid encapsulation materials

Five kinds of liquid encapsulation materials were selected, which were distilled water, sodium chloride, sucrose, calcium chloride, and glycerol. The aqueous solutions of the five materials were prepared at room temperature, and the refractive indexes of the five materials were 1.3325, 1.3800, 1.3840, 1.3850, and 1.3850, respectively. By using Abbe refractometer (WAY-2W, INESA) and controlled thermostat bath (WG-DCZ, INESA), the refractive index of the liquid encapsulation materials in different temperatures were tested. The experimental results showed that when the ambient temperature increased from 25 °C to 85 °C, the refractive indexes of the five solutions changed with temperatures, as shown in Fig. 3. In which, distilled water, sodium chloride solution, and sucrose solution correspond to the lower left coordinate axis (black), calcium chloride solution and glycerol solution correspond to the upper right coordinate axis (red).

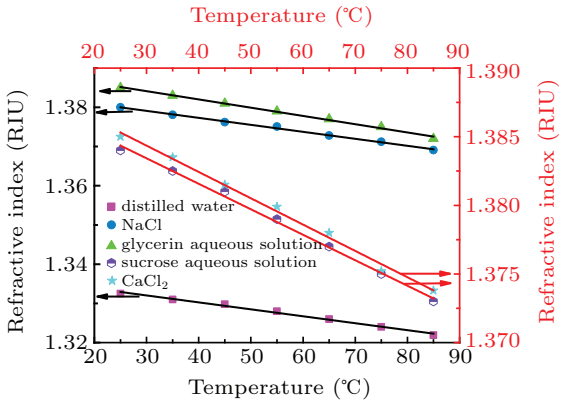


Fig. 3. Experimental data plot of refractive index *versus* temperature for five liquid encapsulation materials (slope is thermo-optic coefficient).

When the ambient temperature increases from 25 °C to 85 °C, the refractive index of distilled water decreases from 1.3325 to 1.3219. After linear filtering, the relationship between the refractive index of the distilled water n_{D} and temperature T is as follows:

$$n_{\mathrm{D}} = -1.77 \times 10^{-4} T + 1.3373. \tag{1}$$

The refractive index of sodium chloride solution decreases from 1.3800 to 1.3691. After linear filtering, the relationship between the refractive index of the sodium chloride solution n_{So} and temperature T is as follows:

$$n_{\mathrm{So}} = -1.78 \times 10^{-4} T + 1.3844. \tag{2}$$

The refractive index of sucrose solution decreases from 1.3840 to 1.3730. After linear filtering, the relationship between the refractive index of the sucrose solution n_{Su} and temperature T is as follows:

$$n_{\mathrm{Su}} = -1.86 \times 10^{-4} T + 1.389. \tag{3}$$

The refractive index of calcium chloride solution decreases from 1.3850 to 1.3738. After linear filtering, the relationship between the refractive index of the calcium chloride solution n_{Ca} and temperature T is as follows:

$$n_{\mathrm{Ca}} = -1.92 \times 10^{-4} T + 1.39. \tag{4}$$

The refractive index of glycerin aqueous solution decreases from 1.3850 to 1.3720. After linear filtering, the relationship between the refractive index of the glycerol solution n_{Gl} and temperature T is as follows:

$$n_{Gl} = -2.11 \times 10^{-4} T + 1.39. \quad (5)$$

In the above five formulas, the slope -1.77×10^{-4}–1.78×10^{-4}, -1.86×10^{-4}–1.92×10^{-4}, and -2.11×10^{-4} are the thermal-optical coefficients of distilled water, sodium chloride solution, sucrose solution, calcium chloride solution, and glycerol solution, respectively. According to Fig. 3, the refractive indexes of the five solutions decrease with the increase of temperatures, and they all have the negative thermal-optical coefficient and good linearity. The thermal-optical coefficients (curve slope) from large to small are glycerol aqueous solution, calcium chloride solution, sucrose solution, sodium chloride solution, and distilled water.

3.2. Performance simulation of fiber SPR temperature sensor with different liquid encapsulation materials

According to the experimental data of five liquid encapsulation materials measured in the previous section, the performance of liquid encapsulation fiber SPR temperature sensor was simulated. The simulation temperature range was set to be 25 °–85 °C, the refractive index of plastic clad fiber core was set to be 1.467, the change of environmental refractive index was set according to the experimental data, and the thickness of gold film was set to be 50 nm. The simulation results of SPR attenuation spectra (resonance valley) of five encapsulation liquids with temperature changes are shown in Fig. 4.

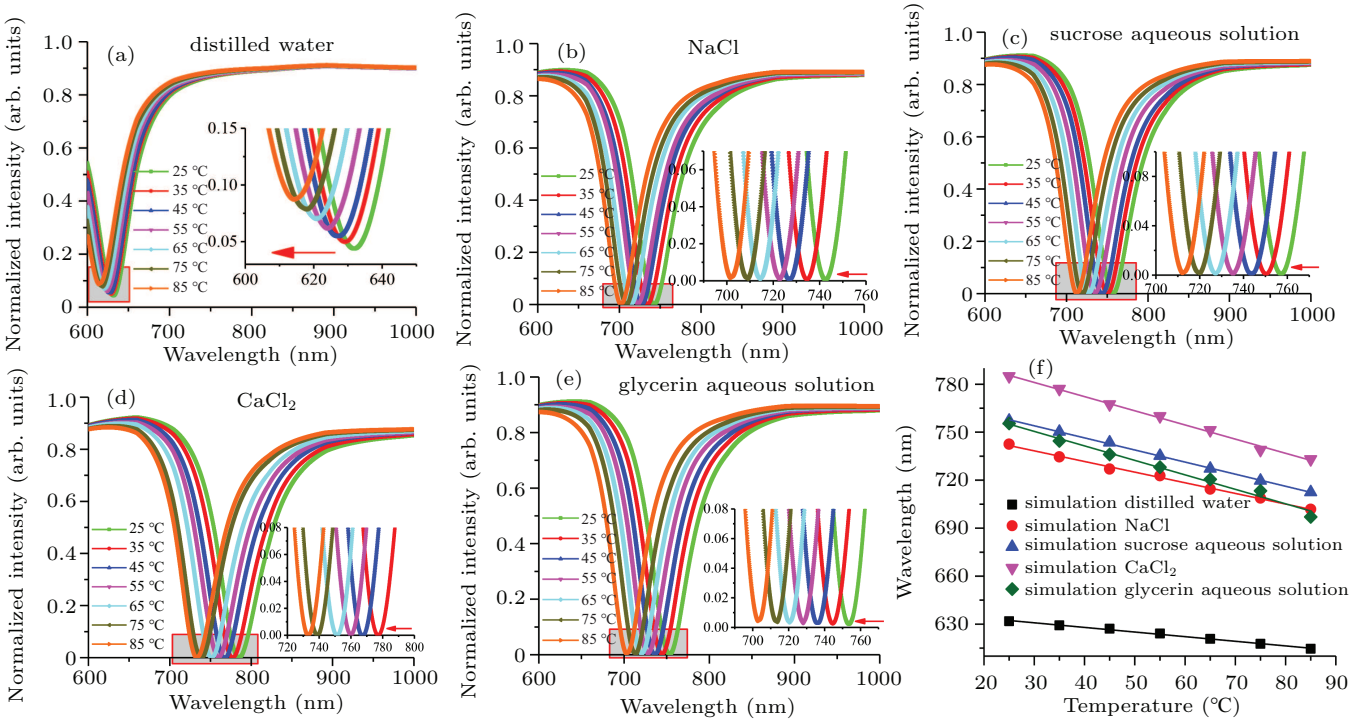


Fig. 4. SPR spectra of the sensing probes sealed with (a) distilled water, (b) sodium chloride solution, (c) sucrose solution, (d) calcium chloride solution, (e) glycerin aqueous solution, (f) the relationship between resonance wavelength and temperature.

It can be seen from the above figure that with the increase of the ambient temperature, the resonance wavelengths of SPR sensors with five kinds of encapsulation liquids all shift to blue (move to short wavelength). According to Fig. 4(f), when the thermo-optic coefficient of the liquid encapsulation materials increases in sequence of distilled water, sodium chloride, sucrose, calcium chloride, and glycerin solution, the sensitivity of the SPR sensor encapsulated by the liquid increases in turn. And with the increase of the initial refractive index of the liquid encapsulation materials, the working dynamic range of the sensor is red shifted (working in the long wavelength band).

4. Experimental results and analysis of fiber SPR temperature sensors with different encapsulation liquids

4.1. Construction of experimental platform

The experimental platform was built as shown in Fig. 5.

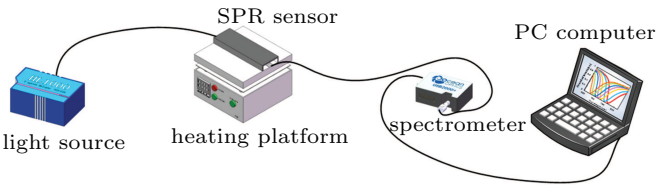


Fig. 5. The sketch diagram of the fiber SPR temperature experiment system.

The light from the wide spectrum light source (HL1000, Wyoptics) was injected into the liquid encapsulated SPR temperature sensor from the left side, and the output light from the right side was injected into the spectrometer (USB2000+, Oceaninsight). The spectrometer was connected with the computer to collect data for subsequent data processing. The fiber SPR temperature sensor probe was placed on a constant temperature heating platform (P-20, Fastelectronics Company) and covered with a heat preservation cover. The constant temperature heating platform increased the ambient temperature from 25 °C to 85 °C with an interval of 10 °C and maintained the constant temperature. The SPR attenuation spectrum of the fiber SRP temperature sensor at each temperature could be acquired and processed in turn.

4.2. Results and analysis

Fiber SPR temperature sensor encapsulated with distilled water, sodium chloride solution, sucrose solution, calcium chloride solution, and glycerin solution were fabricated and tested respectively as shown in Fig. 6. It can be seen from the figure that with the increase of ambient temperature, SPR resonance wavelengths move to short wavelengths.

According to the above experimental results, we summarize and compare the thermal-optical coefficients and refractive index of five different encapsulation liquids changing with the temperature, the working dynamic range and sensing sensitivity of the corresponding sensors are shown in Table 1. It can be seen from the table that, the larger the thermal-optical coefficient of the encapsulation liquid is, the higher the sensitivity of the corresponding temperature sensor is. With the decrease of the refractive index of the encapsulation liquid, the dynamic range of the corresponding temperature sensor moves to shorter wavelength direction. The fiber SPR temperature sensor encapsulated by liquid with different thermal-optical coefficients and refractive indexes has different dynamic ranges and sensitivities, and the overall trend matches well with the simulation results.

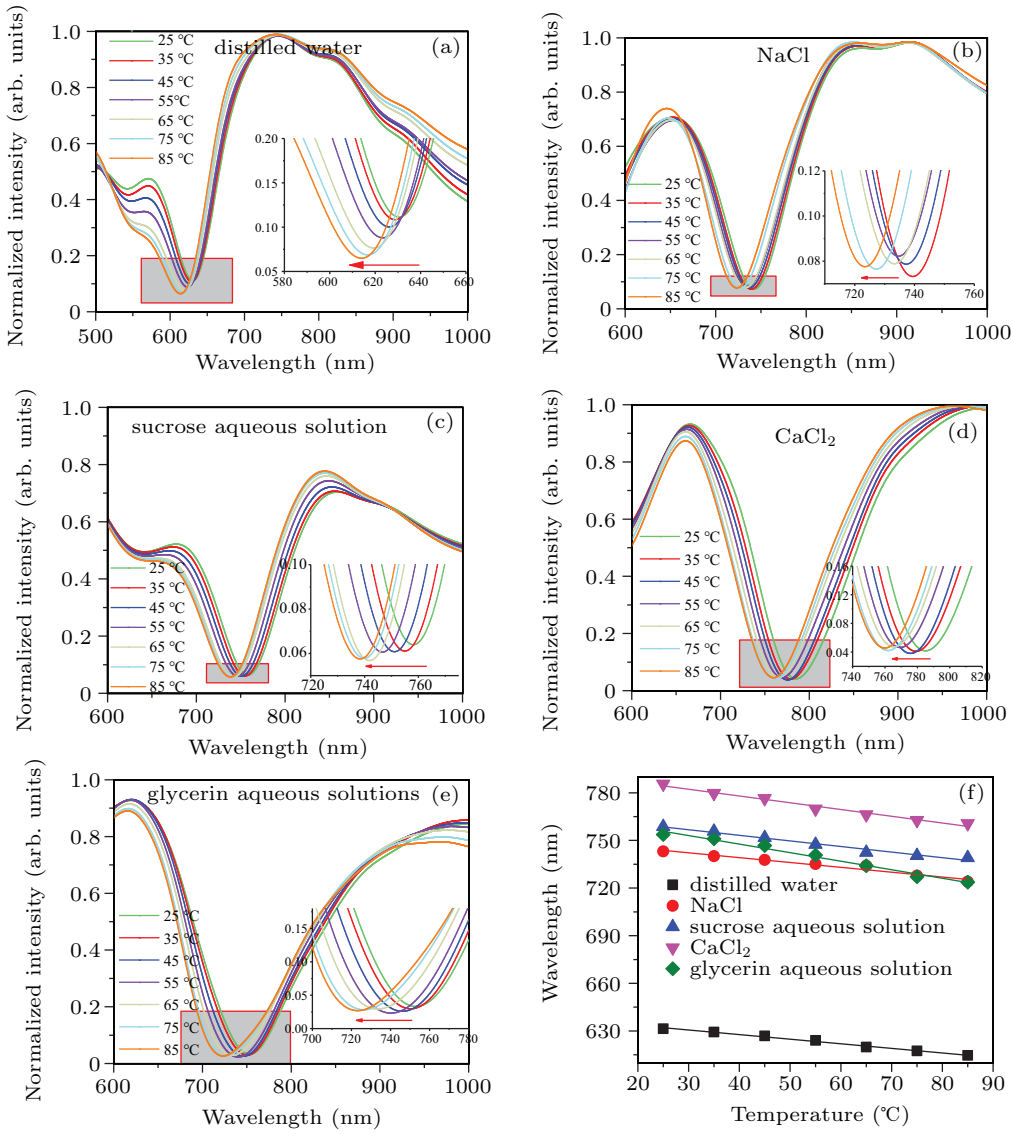


Fig. 6. Testing results of the sensing probes encapsulated with (a) distilled water, (b) sodium chloride solution, (c) sucrose solution, (d) calcium chloride solution, (e) glycerin aqueous solution, (f) relationship between resonance wavelength and temperature.

Table 1. Parameter comparison of different liquids and sensing probes encapsulated with different liquids.

Encapsulation liquids	Thermal-optical coefficients (10^{-4})	Refractive index range (RIU)	Dynamic range (nm)	Sensitivity (nm/°C)
Distilled water	–1.77	1.3325–1.3218	631.4–614.63	–0.2795
Sodium chloride	–1.78	1.3800–1.3691	743.11–724.07	–0.3173
Sucrose	–1.86	1.384–1.373	758.69–739.12	–0.3262
Calcium chloride	–1.92	1.385–1.3738	785.59–760.67	–0.4153
Glycerol	–2.11	1.385-1.372	753.73–723.74	–0.4998

4.3. Temperature response time testing

For the temperature sensor, in addition to sensing sensitivity and dynamic range, it is necessary to study the response time and long-term stability. In order to study the temperature response time characteristics of different encapsulation liquids, we tested the temperature response time of the five solutions. Five fiber SPR temperature sensors sealed in thick quartz tubes (with the diameter of 5 mm) and encapsulated with distilled water, sodium chloride solution, sucrose solution, calcium chloride solution, and glycerin solution were fabricated respectively. During the process of fabrication, the thermocouple was sealed in the quartz tubes to monitor the real-time temperature of the liquid encapsulation material. Five temperature sensing probes encapsulated with different liquid materials were put into the constant temperature water bath with the temperature of 85 °C at the same time The temperature response time at the same ambient temperature was recorded. The SPR data were collected every 30 s, the resonance wavelength was obtained by data processing, and the black curves in Fig. 7 were plotted. Meanwhile, the temperature data of the thermocouple sealed in the quartz tubes were recorded, which were the real-time temperature data of the encapsulation liquid, and the blue curves in Fig. 7 were plotted.

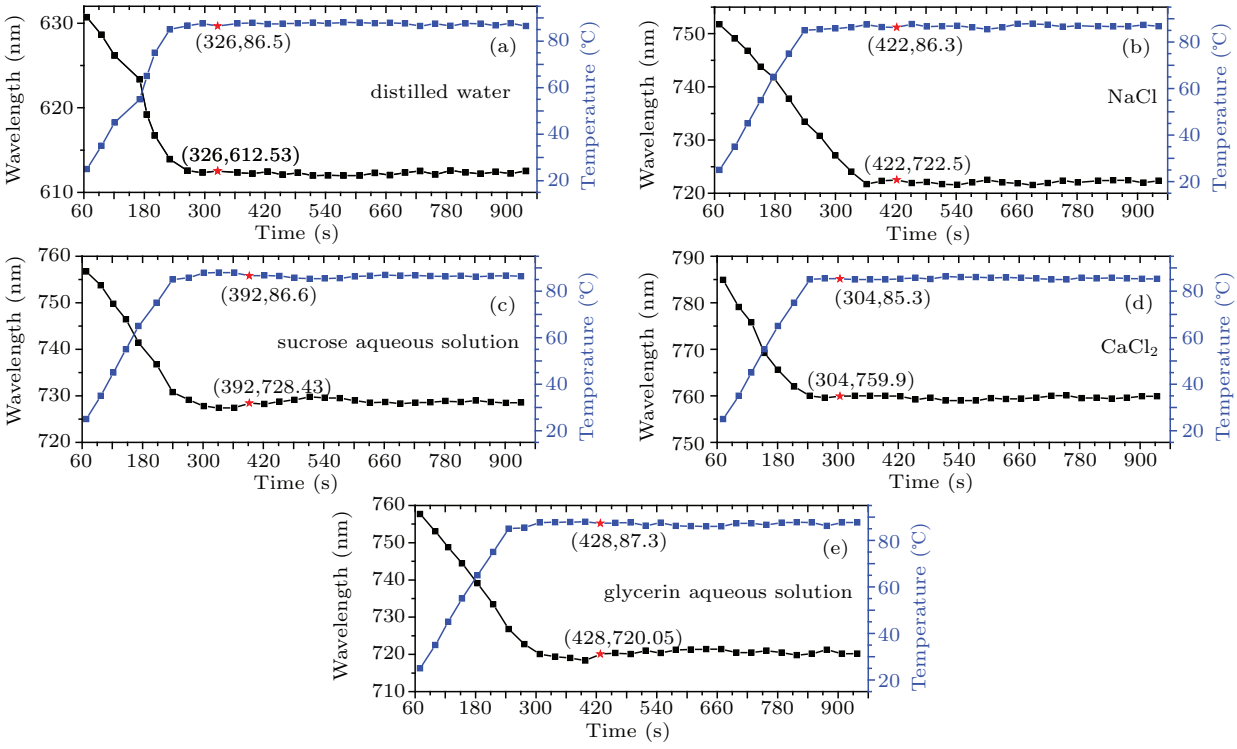


Fig. 7. Temperature response time of (a) distilled water, (b) sodium chloride solution, (c) sucrose solution, (d) calcium chloride solution, (e) glycerin solution.

As shown in Fig. 7, the blue curve represents the real-time temperature of the encapsulation liquid, and the black curve represents the real-time SPR resonance wavelength of the sensor. It can be seen from the figures that the SPR resonance wavelength of the temperature sensor encapsulated with distilled water, sucrose solution, and glycerol solution have good response to the real-time temperature change of the encapsulation solution as shown in Fig. 7(a), 7(c), and 7(e) For the temperature sensor encapsulated with sodium chloride solution, the curve of SPR resonance wavelength changes with time is slower than that of sodium chloride solution, as shown in Fig. 7(b). The reason is that sodium chloride solution is easy

to precipitate crystals at high temperature, resulting in the interference of the refractive index of the solution, which affects the response time of the sensor. For the temperature sensor encapsulated with calcium chloride solution, the curve of SPR resonance wavelength changes with time is faster than that of sodium chloride solution, as shown in Fig. 7(d). The main reason is that calcium chloride dissolves in water and easily generates calcium hydroxide with exothermic phenomenon.

Based on the experiment results above, the dynamic range of the sensing probe encapsulated with distilled water which has a low thermal-optical coefficient is in short wavelength, and dynamic range of the sensing probe encapsulated with glycerin solution which has a high thermal-optical coefficient is in long wavelength, and its sensing sensitivity is higher than the former. Besides, for the temperature sensor encapsulated with sodium chloride solution and calcium chloride solution, the response time of the SPR resonance wavelength has differences with that solution temperature time which leads to the poor accuracy of temperature sensing.

5. Solid material encapsulation and dual -hannel temperature sensing

5.1. Sensing testing of the temperature sensor encapsulated with solid material

Solid material usually has higher thermal-optical coefficient than liquid material, but it also has a higher refractive index. In order to study the performance of fiber SPR temperature sensor encapsulated with solid material, we selected pouring sealant as the solid encapsulation material. Firstly, the refractive index of the pouring sealant changed with the temperature was studied. The AB solution of the pouring sealant were mixed and with the mass ratio of 10:1, the mixture was let-stand until bubbles disappear. Then put it into the incubator and heat it at 60 °C for 2 hours to cure. By using blades, a 1 cm×1 cm solid slice of pouring sealant was took and put into Abbe refractometer. The Abbe refractometer was connected with intelligent constant temperature water tank which was used for the refractive index detection of the pouring sealant at different temperatures. With the temperature increases from 35 °C to 95 °C the refractive index of the pouring sealant decreases from 1.401 to 1.381. As shown in Fig. 8, the slope -3.36×10^{-4} is the thermal-optical coefficient of the pouring sealant after the linear fitting.

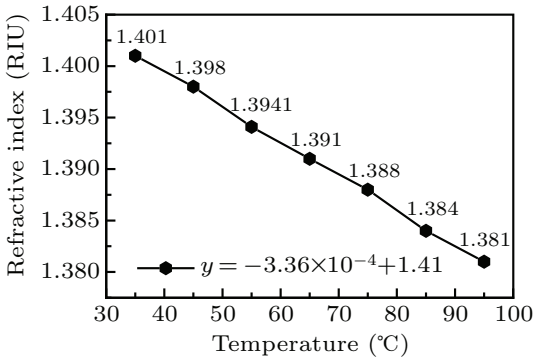


Fig. 8. Experimental data of refractive index of pouring sealant changing with temperatures.

Secondly, the sensing probe encapsulated with solid material was fabricated. Figure 9(a) was practicality picture of the sensing probe, and figure 9(b) was structure chart. The first two steps of the fabrication process of the sensing probe encapsulated with solid material was the same as the sensing probe encapsulated with liquid material as shown in Figs. 10(a) and 10(b). The third step was to cover the gold film with pouring sealant as shown in Fig. 10(c), the encapsulation length was 2 cm.

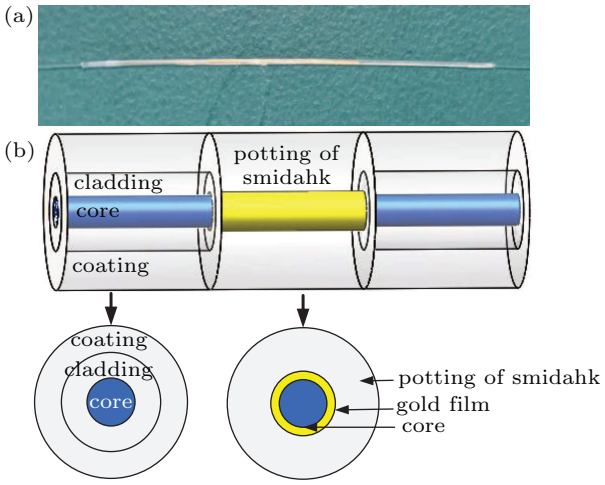


Fig. 9. Solid-encapsulated fiber SPR temperature sensor, (a) practicality picture, (b) schematic diagram.

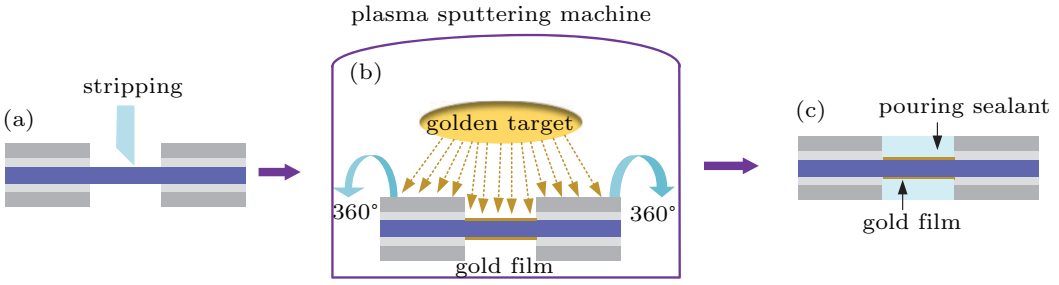


Fig. 10. The fabrication of the solid-encapsulated fiber SPR temperature sensor, (a) mechanical stripping of coating and plastic cladding, (b) ring plating of 50-nm gold film, (c) pouring sealant encapsulation.

Finally, we performed the sensing testing of the solid encapsulated fiber SPR temperature sensor. By using the experimental platform shown in Fig. 5, the sensing probe was tested. As shown in Fig. 11(a), the resonance wavelength of SPR shifts to short wavelength with the increase of temperature. Figure 11(b) shows the curve of SPR resonance wavelength changing with temperature, in which, the sensitivity is −1.85 nm/°C, and the dynamic range is 819.3 nm–710.11 nm. Compared with the liquid encapsulated SPR temperature sensor, its working band is more partial to long wavelength direction.

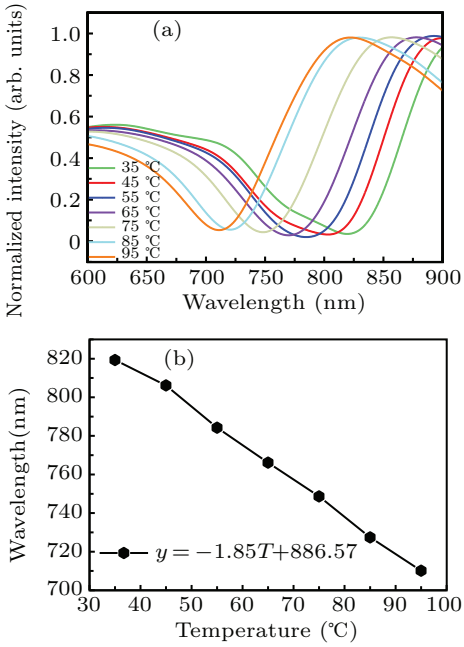


Fig. 11. Solid-encapsulated fiber SPR temperature sensor (a) temperature testing results, (b) SPR resonance wavelengths changing with temperatures.

5.2. Dual-channel SPR temperature sensor based on the cascade encapsulation of solid and liquid

In order to realize the dual-channel temperature detection based on WDM, it is necessary to fabricate two sensing zones on a fiber. And the working band of the two sensing zones should be separated as much as possible, so that the two SPR resonance valleys in the SPR attenuation spectra can be distinguished well. Meanwhile, in order to avoid the difficulty in recognition of the shallower resonance valley, the depth of the two resonance valleys should be as same as possible. In the research process of liquid-encapsulated sensor, we find that the distilled water has lower thermo-optic coefficient and encapsulation detection sensitivity, but its refractive index is lower and works in short wavelength. This makes distilled water be beneficial to cascade with the pouring sealant which has a high refractive index and works in long wavelength to realize the dual-channel sensing. Thus, we selected distilled water worked in the short wavelength as the zone A, pouring sealant worked in the long wavelength as the zone B to realize the dual-channel SPR sensor, and the distance between the two sensing zone was 5 cm. The sensing structure is shown in Fig. 12.

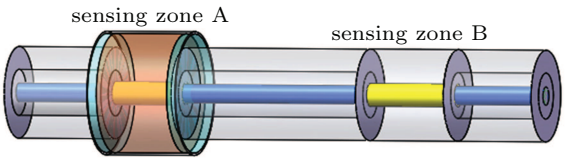


Fig. 12. Solid–liquid-encapsulation cascade dual-channel SPR sensor.

The performance of the cascade dual-channel temperature sensor was tested. As shown in Fig. 13(a), there are two SPR resonance valleys in one measurement, and both of them are blue shifted with the increase of temperature, but the second resonance valley is not easy to identify. In order to optimize the SPR resonance valleys of the two sensing zones, we designed the data processing program. The position of the second resonance valley was found out and marked, then the data were normalized to make the depth of the two resonance valleys become basically the same as shown in Fig. 13(b). It can be seen from the figures that the dynamic range of the sensing zone A is 639.05 nm–616.03 nm, and its temperature detection sensitivity is −0.384 nm/°C. The dynamic range of the sensing zone B is 825.27 nm–719.37 nm, and its temperature detection sensitivity is −1.765 nm/°C.

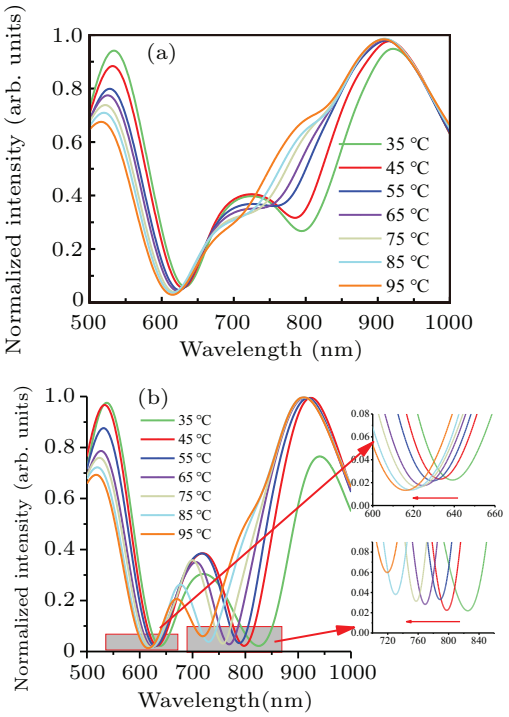


Fig. 13. (a) Testing results of the dual-channel SPR temperature sensor, (b) data processing results of panel (a).

6. Conclusions

In this paper, by studying the effects of five kinds of liquid encapsulation materials on the dynamic working range, tem-

perature sensing sensitivity, and response time of fiber SPR temperature sensor, we employed the distilled water which can make the working wave band in short wavelength to fabricate the liquid encapsulation stage, and the pouring sealant which can make the working wave band in long wavelength to fabricate the solid encapsulation stage. The liquid encapsulation stage and solid encapsulation stage were cascaded to realize the dual-channel fiber SPR temperature sensor, and the temperature detection sensitivities of the two stages are -0.384 nm/°C and -1.765 nm/°C respectively. The proposed fiber SPR sensor employed WDM technology to realize the dual-channel detection, which can be used for temperature compensation, simultaneous measurement of liquid and solid temperature, dual-channel temperature measurement, *etc*. And it has the advantages of simple fabrication, low cost, and high temperature sensitivity, which can be used in fire alarm, industrial manufacturing, and other fields.

References

[1] Wu S, Tan Q, Forsberg E, Hu S and He S 2020 *Opt. Express* **28** 21046
[2] Afcp A, Nmn A, Hmcdp B, Ylc B, Lhmds B, Msp C and Acdsp A 2020 *International Dairy Journal* **108** 104728
[3] Abdelaty M S A 2020 *Journal of Polymers and the Environment* **28** 2599
[4] Ping L 2009 *Appl. Phys. Lett.* **94** 131110
[5] Li B Y, Ni S F, Gao Z T and Wang S M 2014 *Proceedings of the International Society for Optical Engineering* **9297**
[6] Zhu J J, Zhang A P, Xia T H, He S and Xue W 2010 *IEEE Sensors Journal* **10** 1415
[7] Park M, Lee S, Ha W, Kim D K, Shin W, Sohn I B and Oh K 2009 *IEEE Photon. Technol. Lett.* **21** 1027
[8] Jiang L, Yang J, Wang S, Li B and Wang M 2011 *Opt. Lett.* **36** 3753
[9] Zhang X, Peng W and Zhang Y 2015 *Opt. Lett.* **40** 5658
[10] Li W C, Yuan Y G, Yang J and Yuan L B 2019 *Opt. Express* **27** 14675
[11] Yang T, He X, Ran Z, Xie Z, Rao Y, Qiao X, He Z and He P 2018 *Materials* **11** 1867
[12] Xu J, Liu Y G, Wang Z and Tai B 2010 *Appl. Opt.* **49** 492
[13] Yan B, Sun L, Luo Y, Yang L and Peng G D 2019 *Sensors* **19** 5211
[14] Zhang S, Deng S, Geng T, Sun C and Yuan L 2020 *Opt. Laser Technol.* **126** 106121
[15] Wang Q, Du C, Zhang J, Lv R and Zhao Y 2016 *Opt. Commun.* **377** 89
[16] Zhu Z, Liu L, Liu Z, Yu Z and Zhang Y 2017 *Opt. Lett.* **42** 2948
[17] Zhao Y, Deng Z and Hu H 2015 *IEEE Transactions on Instrumentation and Measurement* **64** 3099
[18] Wu S, Tan Q, Forsberg E, Hu S and He S 2016 *Opt. Express* **24** 10904